Nonlinear scattering in photonic crystals having dislocations with fractional topological character and multiple dislocations

Liran Naor,[1,*] Shani Sharabi,[1] Irit Juwiler,[2] and Ady Arie[1]

[1]*Department of Physical Electronics, Fleischman Faculty of Engineering, Tel Aviv University, Tel Aviv 6997801, Israel*

[2]*Department of Electrical and Electronics Engineering, Sami Shamoon College of Engineering, Ashdod 77245, Israel*

(Received 18 February 2015; published 21 May 2015)

The spectrum of the second harmonic signal generated in quadratic nonlinear photonic crystals, having different types of edge dislocations, was studied theoretically and experimentally. In the case of a dislocation with a fractional topological charge, we observed an asymmetric spectral conversion efficiency response, where the degree of asymmetry depends on the value of the fractional charge. Moreover, we have found that the conversion efficiency spectrum exhibits a periodic dependence on the topological charge value. In addition, nonlinear photonic crystals with multiple edge dislocations were studied. We show that for any number of dislocations characterized by even topological charge, the nonlinear spectral response will be identical to the response of the ideal, dislocation-free structure. This is a generalization of a previous observation that was made for crystals with a single even charge dislocation. Furthermore, for any number of dislocations with odd topological charge, two new peaks of maximal efficiency are observed in the second harmonic spectrum, in addition to a series of local efficiency peaks that are governed by the total number of dislocations. This is also a generalization of a previous observation that was made for a single dislocation case having an odd topological charge.

DOI: 10.1103/PhysRevA.91.053841 PACS number(s): 42.65.Ky, 61.72.Ff, 61.72.Hh, 61.72.Lk

I. INTRODUCTION

Dislocations have an enormous importance in the study of material properties as well as in studying the propagation dynamics of waves in matter. First, the presence of dislocations in a solid-state material can influence its mechanical, electrical, thermal or optical properties, as compared to its perfect, dislocation-free counterpart. Specifically, dislocations play a significant role in the understanding of the microscopic nature of mechanical deformations that a material can perform through the arrangement of dislocations [1,2]. In addition, dislocations are used in the study of the electrical conductivity in conductive materials through the transport of electrons via dislocation cores, or through the movements of the dislocations [3–5]. Furthermore, dislocations are also used in the study of the thermal conductivity of materials through the interaction between acoustic phonons and dislocations [6–9]. Therefore, extensive studies on the scattering of electron, phonon, and electromagnetic waves from dislocations were carried in order to understand the influence of dislocations on the material's properties.

Secondly, in addition to structural dislocations in crystals, dislocation lines and dislocation effects can also be present in the wave fronts of different types of waves [10–12]. Such wave dislocations are often created when the wave scatters from a structural dislocation of a crystal. Therefore, the interaction between dislocations and waves in matter raises great interest and as a result different types of physical systems that contain topological dislocations were studied. For instance, one may refer to the naturally formed topological dislocations in self-assembled soft-matter quasicrystals [13], which provide a platform for the fundamental study of quasicrystals and their applications in the field of photonics. In addition, topological dislocations were produced in photonic structures. As an example, the transport of matter-wave solitons was studied in optical lattices that contain topological dislocations [14] and the scattering of light from dislocation sites in photorefractive nonlinear photonic quasicrystals was observed [15–17]. Scattering of waves from dislocations is often used to generate vortex beams, carrying orbital angular momentum [18–20].

Dislocations were also studied in quadratic nonlinear photonic crystals. These are crystals in which the sign of the quadratic nonlinear susceptibility is modulated in an ordered fashion, while the linear susceptibility, and thereby the refractive index, remains constant and uniform throughout the entire crystal [21]. In this case, the effect of the dislocation is observed at the second harmonic of the input beam. Two different types of dislocations were studied until now: continuous dislocations which are present along the entire nonlinear photonic crystal [22,23] and local defects [24,25]. Nonlinear scattering from quadratic nonlinear crystals with dislocations was recently used to generate [26] and manipulate [27] the orbital angular momentum of the scattered second harmonic light. In this paper we shall concentrate on a specific local defect—the edge dislocation. It is manifested by a cumulative addition of modulation periods that appear only on one side of the dislocation's core, and therefore do not extend through the entire crystal length. In our case, the designed structures in the crystals contain local topological edge dislocations with a fork-shape (or a Y-shape) form. The degree of deviation from the ordered periodical state, by the edge dislocation, is characterized by a topological property of the dislocation—the topological charge. This topological charge can be determined for a given dislocation by enclosing a loop around its position, count the number of modulation

*lirannao@mail.tau.ac.il

periods when moving on one side of the dislocation's core, and subtract the number of modulation periods when moving on the other side of the core. This practical method allows one to determine the value of the topological charge if it is an integer number. However, we can also consider defects with a fractional charge by simply using a noninteger value of the topological charge.

Recently, the nonlinear scattering from quadratic nonlinear photonic crystals having edge dislocations was examined. It was found that the spectral response of the nonlinear conversion efficiency is governed by the parity of the dislocation's topological charge value [28]. We note that the dislocation-free reference case is of a nonlinear crystal with a periodic (or a quasiperiodic) modulation of its second-order nonlinear coefficient, which is widely used for quasi-phase-matched frequency conversion processes. Adding a dislocation with an odd topological charge in the middle of the structure nulls the conversion efficiency of the otherwise optimally phase-matched wavelength. Nevertheless, high conversion efficiency is now achieved at new wavelengths that exhibited low efficiency without the dislocation. In contrast to that, a dislocation with an even topological charge has a negligible effect on the spectral conversion efficiency curve.

So far, only nonlinear photonic crystals having a single dislocation with an integer topological charge were studied. This raises new questions that were not addressed up until now—what happens for dislocations with a fractional charge? What is the effect on the scattered nonlinear signal? What will happen if there are multiple dislocations and not only one? Here we report for the first time the theoretical and experimental study of these effects. For dislocations having a fractional charge, an asymmetric spectral conversion efficiency response is observed, where the degree of asymmetry depends on the value of the fractional topological charge. The efficiency spectrum (as a function of the phase mismatch) exhibits periodic dependence on the topological charge. In the case of multiple dislocations, we show that the nonlinear spectral response for any number of dislocations, characterized by an even topological charge, is identical to the response of the ideal, dislocation-free structure. Furthermore, for any number of dislocations with an odd charge, two new global peaks of maximal efficiency are observed in the second harmonic spectrum. Additional local peaks are observed in the efficiency spectrum between the two global peaks. The number of these local peaks is determined by the number of dislocations in the patterned structure. These results represent generalization of phenomena that were previously observed with a single, integer charge dislocation [28].

The paper is organized as follows. In Sec. II, we present the main aspects of the model which was used in order to realize the nonlinear interaction in the studied configurations. In Sec. III, we describe the fabricated nonlinear photonic crystal structures. In Sec. IV, we study the effects of a fractional charge dislocation on the spectral nonlinear second harmonic conversion efficiency, whereas in Sec. V, we study the effects of multiple dislocations on the nonlinear spectral response. Finally, in Sec. VI, we conclude and suggest directions for future work in the field of nonlinear scattering from dislocations.

II. THE THEORETICAL MODEL

Efficient frequency doubling of a pump beam at the fundamental frequency (FF) in a quadratic nonlinear crystal to its second harmonic (SH) frequency requires phase matching between the two interacting waves. This can be achieved by quasi-phase-matching, i.e., periodic modulation of the sign of the second-order nonlinear susceptibility at a spatial frequency which is identical to the phase mismatch Δk, between the interacting waves [21,29]. In this case, the nonlinear crystal can be considered an ideal one-dimensional nonlinear photonic crystal. Only one particular pump wavelength will be quasi-phase-matched with the maximal conversion efficiency at the output of the crystal. Hence there is a single global peak of maximum efficiency in the spectral efficiency curve, which indicates that a maximum amount of energy was converted from the FF wave to the SH wave. We can now consider what happens if dislocations are introduced in this structure. As mentioned above, the case of a single edge dislocation having an integer topological charge was studied recently [28].

Here we examine a more general case in which the second-order nonlinear susceptibility expression of a periodic structure contains any number and any type of topological edge dislocations. In this case, the two-dimensional pattern can be written as

$$\chi^{(2)}(X,Y) = 2d_{ij}\,\mathrm{sgn}\left[\cos\left(\frac{2\pi}{\Lambda}X + \sum_{m=1}^{N} l_m \Phi_m(X,Y)\right)\right], \tag{1}$$

where d_{ij} is a proper element of the second-order nonlinear susceptibility tensor, which contribute the most to the nonlinear coupling between the two waves. The left term inside the cosine function provides a periodic structure with a profile of a carrier wave. Its wave number enables to overcome the phase mismatch between the FF and the SH waves. Λ is the period length of the alternation of the sign of the nonlinear coefficient, required for quasi-phase-matching. The right term inside the cosine function is responsible for embedding dislocations inside the periodic structure. l_m represents the topological charge of the m^{th} dislocation (which can be either an integer or a fractional number), $\Phi_m = \arctan(X_m/Y)$ is the azimuthal angle between the beam's propagation direction in the crystal (the X axis) and one of its perpendicular directions in the crystal (the Y axis), and N is the total number of dislocations that are embedded in the structure. In our designs, we placed the dislocations in equally spaced distances from each other and with respect to the crystal's longitudinal limits through the definition of $X_m = X - [1/2 - m/(N+1)]\,L$, where L is the length of the crystal along the X axis. It should be noted that if all the values of l_m are equal to zero, then one gets a structure with an ideal periodic modulation without any dislocations. The case of structures that contain a single dislocation, characterized by a fractional charge, is demonstrated at the bottom part of Fig. 1. In these structures, $N = 1$, and the difference between each dislocation is reflected in a different fractional value of the topological charge, where in (a) $l = 1/2$, in (b) $l = 3/4$, and in (c) $l = 3/2$. The case of dislocations characterized by integer charges is demonstrated at the bottom part of Fig. 2. In this structure, $N = 2$, and

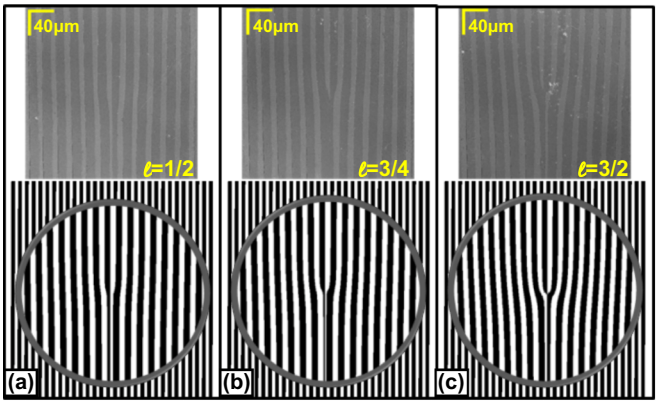

FIG. 1. (Color online) Microscope pictures of the different topological edge dislocations that were implemented in crystals where each one of them contained one dislocation positioned in the middle of the periodic structure relative to the crystal's edges. The bottom part of each figure presents, as an illustration of the designs, a magnification of the area where a dislocation was positioned in the structure. (a)–(c) Comparisons between the fabricated and the designed structures.

the difference between each dislocation is reflected in a different integer value of the topological charge. Therefore, the multiplication $l_m \cdot \Phi_m$ generates a different cumulative addition of modulation periods on one side of the dislocation's core, that eventually leads to a particular shape of an edge dislocation. For instance, in the right illustrated dislocation in Fig. 2, the difference between the number of modulation periods when moving on one side of the core, and this number on its other side, is equal to 2. On the other hand, in a fractional charge dislocation, this difference is not considered as an integer number.

The spectral response of the nonlinear conversion efficiency due to the propagation of a fundamental pump beam in a nonlinear medium was calculated using the Split-Step Fourier method [30]. The nonlinear interaction inside the crystal between the incident FF pump beam, with angular frequency ω_1, and the generated SH beam, with angular frequency $\omega_2 \equiv 2\omega_1$, is governed by two coupled-amplitude equations. Under the approximation of slowly varying amplitudes for the FF wave, $A_1(X,Y,Z)$, and for the SH wave, $A_2(X,Y,Z)$, these equations in Fourier space for monochromatic beams are given by

$$\frac{d\tilde{A}_1}{dX} + \frac{i\left(K_Y^2 + K_Z^2\right)\tilde{A}_1}{2k_1} = \kappa_1 \int_{-\infty}^{\infty}\int_{-\infty}^{\infty} dY\,dZ\,A_2 A_1^{*}\chi^{(2)} e^{-i\vec{G}_1\cdot\vec{r}}, \tag{2a}$$

$$\frac{d\tilde{A}_2}{dX} + \frac{i\left(K_Y^2 + K_Z^2\right)\tilde{A}_2}{2k_2} = \kappa_2 \int_{-\infty}^{\infty}\int_{-\infty}^{\infty} dY\,dZ\,A_1^2\chi^{(2)} e^{-i\vec{G}_2\cdot\vec{r}}, \tag{2b}$$

where $\tilde{A}_1 = \tilde{A}_1(X,K_Y,K_Z)$ and $\tilde{A}_2 = \tilde{A}_2(X,K_Y,K_Z)$ are the two-dimensional Fourier transforms of A_1 and A_2, respectively, and K_Y, K_Z are the spatial frequencies in the transverse plane. The coupling constants are $\kappa_1 \equiv i\omega_1^2/k_1c^2$ and $\kappa_2 \equiv i\omega_2^2/2k_2c^2$, where k_1 and k_2 are the magnitudes of the wave

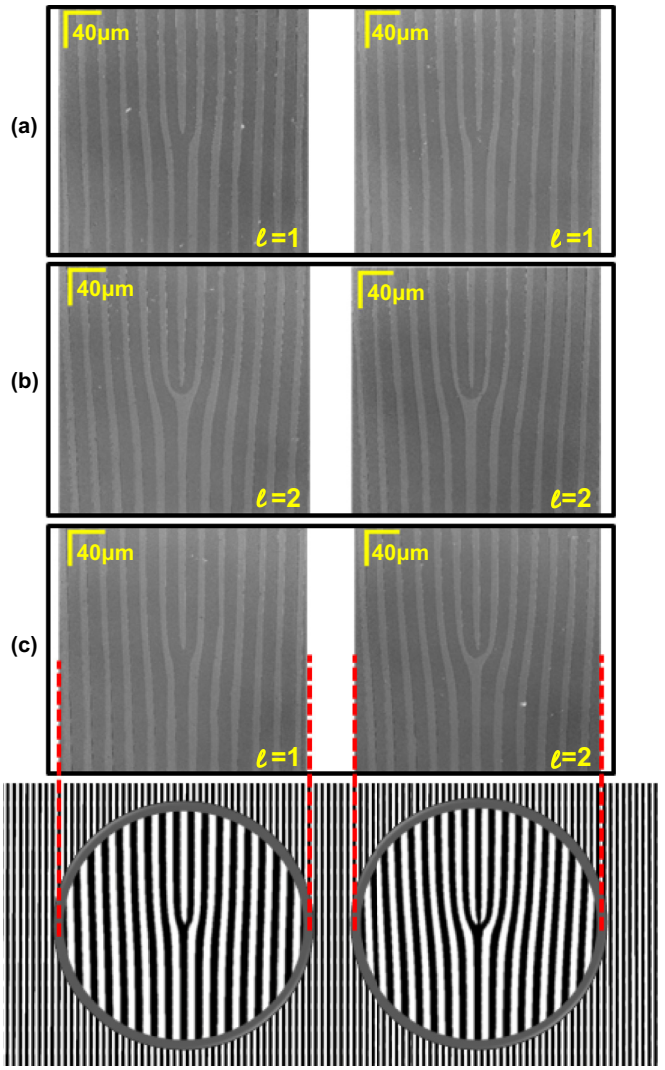

FIG. 2. (Color online) Microscope pictures of the different topological edge dislocations that were implemented in crystals that contained a pair of dislocations. An illustration of the designed structure is presented schematically at the bottom of the figure for one of the crystals which consists of a periodic structure, and the two dislocations in the structure are magnified. The left dislocation is located after one-third of the crystal's edge relative to the total length of the crystal and has a topological charge of $l = 1$. The right dislocation is located after two-thirds of the edge and has a topological charge of $l = 2$. (a)–(c) The three topological charge configurations that were examined experimentally. The fabricated dislocations in (c) can be compared with the illustration of the design (connected with the red dashed line).

vectors of the FF and SH beams in the direction of propagation of the waves. In addition, we defined $\vec{G}_1 \equiv (\Delta k, K_Y, K_Z)$ and $\vec{G}_2 \equiv (-\Delta k, K_Y, K_Z)$ where $\Delta k \equiv 2k_1 - k_2$ is the phase mismatch for a colinear interaction between the two waves. The right term on the left-hand side of each of these equations governs the diffraction of the beams inside the crystal under the paraxial approximation. The terms on the right-hand side of each of the equations govern the nonlinear interaction. If the nonlinear coupling is weak such that the pump intensity is nearly unchanged during the propagation

in the crystal, Eq. (2b) can be solved by integrating over the crystal's length also in the longitudinal direction. In this case, the spectrum of the SH amplitude, $\tilde{A}_2(\Delta k, K_Y, K_Z)$, is proportional to the Fourier transform of the modulation structure, $\tilde{\chi}_2^{(2)}(\Delta k, K_Y, K_Z)$.

III. FABRICATED CONFIGURATIONS AND EXPERIMENTAL SETUP

In order to test experimentally the effects of embedding a topological edge dislocation with a fractional topological charge or of multiple topological edge dislocations with integer topological charges in nonlinear crystals, we designed and fabricated crystals with several two-dimensional modulation patterns of the second-order nonlinear susceptibility. The designed patterns were implemented in stoichiometric lithium tantalite (SLT) nonlinear crystals with length dimensions of 1 cm × 1 mm × 0.5 mm by using the technique of electric field poling. In this fabrication process an electric field pulse was applied on metallic patterned electrodes, that match to the desired structures, after they were placed on the crystal's *X*-*Y* surfaces [21]. In total, six structures which included topological edge dislocations were fabricated, all of them with a central period length of $\Lambda = 21\ \mu$m. Three of them included a dislocation with a fractional topological charge of $l = 1/2$, $l = 3/4$, and $l = 3/2$, respectively. The other three structures were prepared in order to study the effects of multiple dislocations with integer topological charges. Hence, each structure contained a pair of dislocations: The first corresponds to dislocations with topological charges of $l_1 = 1$ and $l_2 = 1$, the second corresponds to topological charges of $l_1 = 2$ and $l_2 = 2$, and the third corresponds to topological charges of $l_1 = 1$ and $l_2 = 2$. These three pairs of topological charges were chosen in order to cover all the possible combination cases of parities in structures that contain two dislocations. For the benefit of observing the modulation patterns of the second-order nonlinear susceptibility, the surfaces of the crystals on the *X*-*Y* plane were selectively etched. The etched surface was then measured using a scanning confocal microscope. The six fabricated patterns are presented in Figs. 1 and 2.

In the experiment, the FF pump beam was produced by a tunable CW diode laser that was amplified by an erbium doped fiber amplifier (EDFA). The wavelength of the pump beam was set to values in the range of 1.54–1.56 μm in order to obtain the nonlinear spectral response. To get a significant nonlinear conversion efficiency we aimed to exploit the largest element d_{33} of the second-order susceptibility tensor of an SLT crystal. Therefore, an interaction of an e-ee SH generation process was achieved by polarizing the pump beam linearly along the *Z* axis of the crystal. The pump beam was focused to the center of the crystal, with a waist radius of 60 μm. The phase-matching temperature of 50 °C was reached by placing the crystals in an oven connected to a temperature controller. For every wavelength of the FF pump beam, the power of the generated SH beam was measured after the output facet of the crystal while the residual FF beam was blocked before the detector by a spectral filter. Sensitive detection was achieved by chopping the FF beam at 1 kHz and demodulating the SH signal using a lock-in amplifier. The spectral conversion efficiency was deduced by measuring the incident power of the FF pump for each wavelength. The experimental setup is shown in Fig. 3.

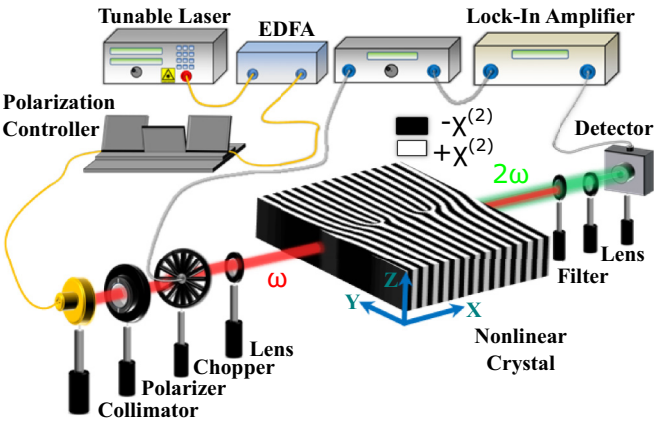

FIG. 3. (Color online) The experimental setup. The red (dark gray) and green (light gray) colors of the beams illustrate the pump and SH beams, respectively.

IV. FRACTIONAL CHARGE EGDE DISLOCATION EFFECTS

Let's consider first the effect of a single dislocation with a fractional topological charge. We present in Fig. 4 numerical calculation results of the spectral response curves for the nonlinear SH conversion efficiency as a function of the pump wavelength, for structures that contain a single topological edge dislocation, with different values of the topological charge. The nonlinear conversion efficiency curves that are shown in the leftmost column [Figs. 4(a), 4(e), and 4(i)] appear when propagating along a crystal with a modulation structure that includes a topological dislocation with an integer, even or odd, topological charge. The case of a single dislocation having an integer charge was recently reported [28]. Here we extend the analysis to include a topological dislocation with a fractional topological charge. Thus, we provide a more complete picture for the behavior of the nonlinear response by looking also at the cases that exist in between the configurations with an even or an odd topological charge dislocation. As can be seen from the simulation results, the nonlinear efficiency response curves show that an asymmetry appears in the spectral response and in particular in the peaks in which we get the maximum SH conversion efficiency. Moreover, the nonlinear response exhibits a periodic behavior where the symmetry, the asymmetry, and the periodicity are determined by the topological charge of the single edge dislocation. As for the nonlinear spectral response, our reference is the simple periodic structure without a dislocation [that is, the case with $l = 0$ in Fig. 4(a)], which exhibits a single significant global peak of maximum conversion efficiency at the wavelength of 1.55 μm. This is the FF quasi-phase-matched wavelength of the dislocation-free crystal. All the curves were normalized such that the maximum conversion efficiency is considered to be 1 for the wavelength that was originally designed to show the maximum conversion efficiency without the dislocation. Progressing to the right in the figure [Figs. 4(b)–4(d)], above $l = 0$, the global peak is now shifted towards lower wavelengths during a decrease in

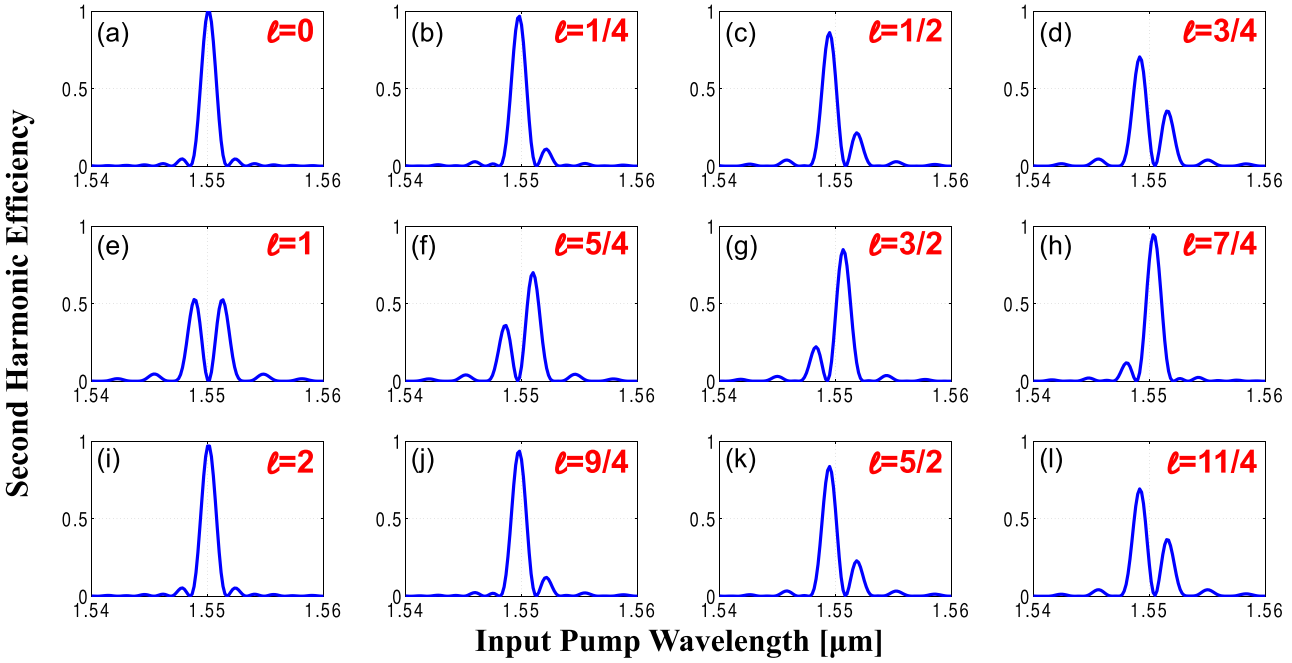

FIG. 4. (Color online) SH conversion efficiency as a function of the input pump wavelength after the propagation through structures that include a single dislocation with a different value of the topological charge.

the efficiency, while a new local peak of efficiency emerges above the reference wavelength of 1.55 μm. Therefore, the existence of a dislocation with a fractional topological charge leads to the appearance of an asymmetry in the peaks of the spectral response curves. This trend continues gradually with increasing values of the fractional charge. When we reach the odd integer value of $l = 1$ [in Fig. 4(e)] these two peaks exhibit identical efficiency. In this case an optimal conversion efficiency is achieved symmetrically at two new FF pump wavelengths, which exhibit low efficiency without the dislocation. In addition, the conversion efficiency of the originally phase-matched wavelength drops to zero. This spectral response is typical to structures that include a dislocation with an odd topological charge [28]. Further increase of the fractional charge beyond the $l = 1$ value [Figs. 4(f)–4(h)], strengthens the right peak above the reference wavelength of 1.55 μm while its position is shifted to the left, towards lower wavelengths. At the same time, the peak to the left of the wavelength of 1.55 μm is getting lower. Thus, the asymmetry in the spectral response appears again. When we get to the case where $l = 2$ [Fig. 4(i)], it can be seen that one period of the spectral response construction is completed where again the spectral SH efficiency curve has one global peak of maximum conversion efficiency at the wavelength of 1.55 μm. This symmetric spectral response is typical to structures that include a dislocation with an even topological charge [28]. By moving forward to cases with higher topological charges [Figs. 4(j)–4(l)], above the case where $l = 2$, one can see that the spectral response curves maintain their shapes repeatedly relative to the topological charge cases between $l = 0$ and $l = 1$ [Figs. 4(b)–4(d)]. Thus, we can predict the nonlinear spectral response after propagating through structures that include a dislocation characterized by any topological charge. Moreover, these results show what are the relations between relative peak values of maximum conversion efficiencies for different cases of the topological charge.

Experimental results for the spectral nonlinear SH conversion efficiency are shown in Fig. 5 for the crystals with the structures shown in Fig. 1, having fractional charges of $l = 1/2$, $l = 3/4$, and $l = 3/2$. These structures represent the cases that were numerically simulated and shown in Figs. 4(c), 4(d), and 4(g). We measured these three structures in order to experimentally study the effects of a dislocation with a fractional topological charge on the nonlinear process. For each one of these three structures, every nonlinear response curve that was obtained by measurements or by simulations, as is presented in Fig. 5, was separately normalized according to its maximum. In order to compare between the measured nonlinear response curves and the curves obtained by numerical simulations we had to shift up the simulation curves by approximately 0.5 nm. This spectral offset may be caused by inaccuracies in the assumed Sellmeier equation [31] as well as by experimental inaccuracies in determining the pump's wavelength or the crystal's temperature. The measured nonlinear response curves show good correspondence with the curves obtained by numerical simulations. One may notice that the two spectral response curves for the dislocations with $l = 1/2$ and $l = 3/2$ [Figs. 5(a) and 5(c)] exhibit a mirror symmetry, which demonstrates a difference of half a cycle between the curves of these two cases when a full cycle is completed for the case with $l = 5/2$. In addition, we examined the relative conversion efficiencies at the peaks for each of the two structures that included a dislocation with a topological charge of $l = 3/4$ and $l = 3/2$ with reference to the case of a dislocation with $l = 1/2$. For the structure that included a dislocation with $l = 3/4$, the measured relative conversion efficiency at the peak was $\eta_{\max}(l = 3/4)/\eta_{\max}(l = 1/2) = 0.87$, while the one obtained in simulation was $\eta_{\max}(l =$

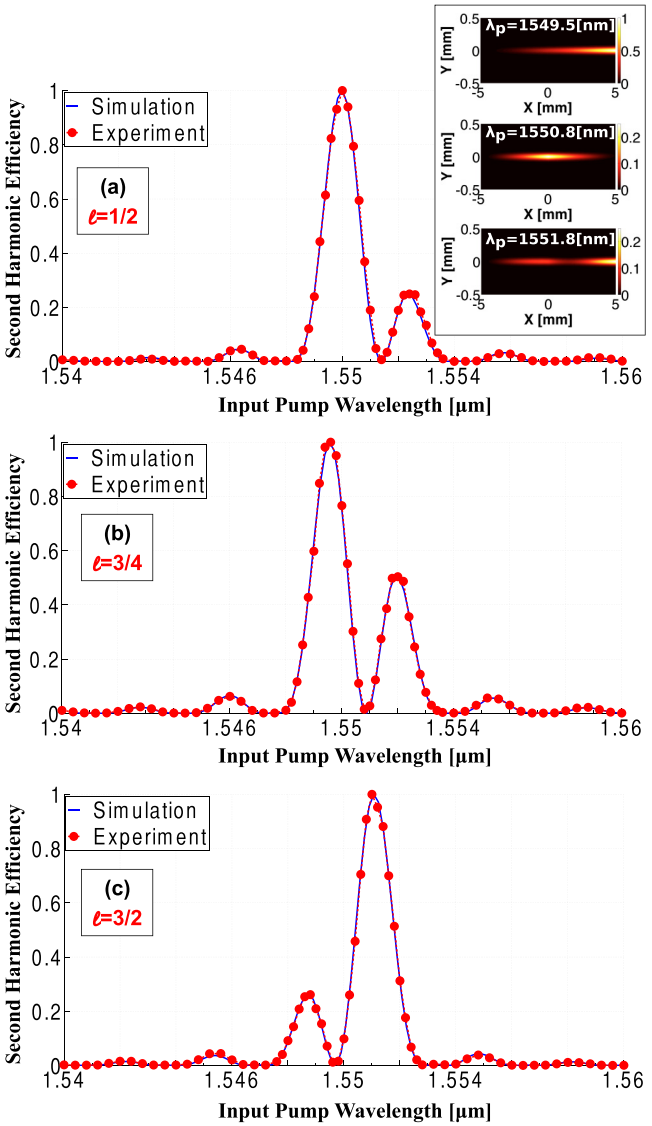

FIG. 5. (Color online) Comparison between the measured and the simulated spectral SH conversion efficiency curves for structures that contained a dislocation with a fractional topological charge of (a) $l = 1/2$, (b) $l = 3/4$, and (c) $l = 3/2$.

$3/4)/\eta_{\max}(l = 1/2) = 0.82$. For the structure that included a dislocation with $l = 3/2$, the measured relative conversion efficiency at the peak was $\eta_{\max}(l = 3/2)/\eta_{\max}(l = 1/2) = 1.07$, while the one obtained in simulation was $\eta_{\max}(l = 3/2)/\eta_{\max}(l = 1/2) = 0.99$. These results also show good agreement between the experimental measurements and the numerical simulations. The insets in Fig. 5(a) show simulations of the evolution of the generated SH intensity inside the structure with $l = 1/2$ as a result of an energy exchange between the propagated FF pump beam and the SH beam, for selected wavelengths of the pump. For pump wavelength of 1549.5 nm, a cumulative construction of the SH leads to the left global peak in the spectral conversion efficiency curve. For pump wavelength of 1550.8 nm, destruction of the generated SH starts at the center of the structure, thereby completely nulling the SH output power. This occurs as a result of a full back-conversion phenomenon, in which the generated SH energy is fully converted back to the original FF energy, when the beam reaches to the dislocation and propagates through the remaining half of the crystal. For pump wavelength of 1551.8 nm, a recovery of the generated SH intensity occurs after passing the dislocation, which leads to a buildup of the SH intensity and to the right local peak in the phase-matching spectrum.

V. MULTIPLE EDGE DISLOCATIONS EFFECTS

So far, we have considered a single edge dislocation. Now we shall examine the effects of multiple dislocations. In Fig. 6 we present the experimental measurements of the SH spectrum in crystals that contained two dislocations with integer topological charges, as is described in Fig. 2.

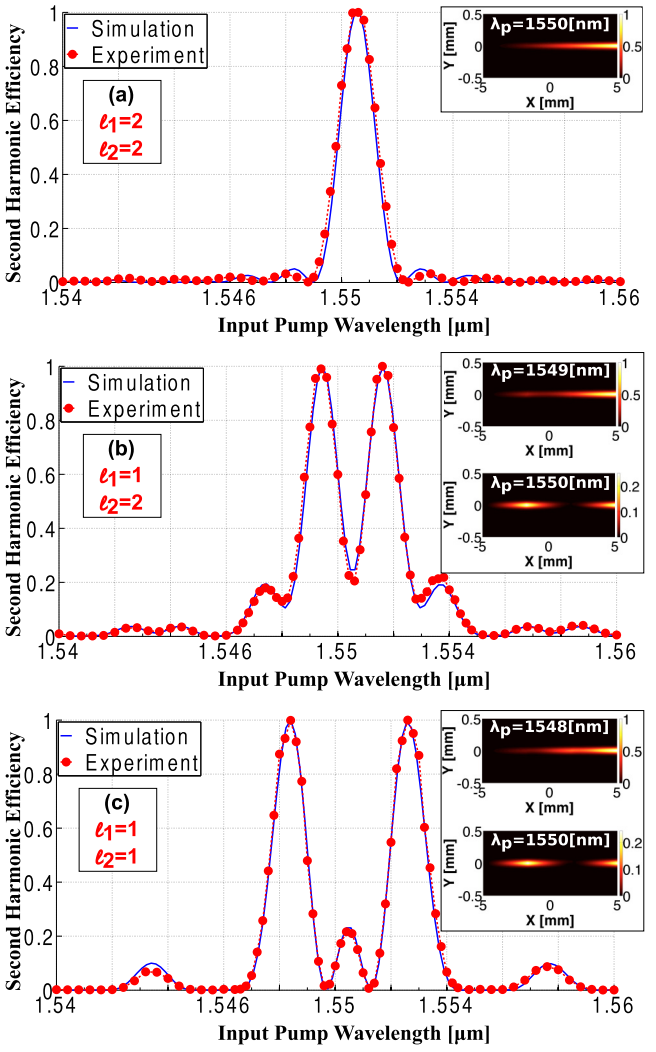

FIG. 6. (Color online) Comparison between the measured and the simulated spectral SH conversion efficiency curves for structures that contained two dislocations with integer topological charges of (a) $l_1 = 2$ and $l_2 = 2$, (b) $l_1 = 1$ and $l_2 = 2$, and (c) $l_1 = 1$ and $l_2 = 1$. The insets in (a), (b), and (c) show simulations of the formation process of the SH intensity inside the crystals, during the propagation of a pump beam for selected wavelengths. The cases of cumulative construction, destruction, and recovery of the SH intensity inside the structures that include different dislocations are demonstrated.

These crystals were fabricated and measured for testing the effects of multiple dislocations on the nonlinear conversion spectrum. The nonlinear response curves that were obtained by measurements or by simulations, as is presented in Fig. 6, were separately normalized according to their maximum. The same spectral offset of approximately 0.5 nm was taken into account for the comparisons between the measured and the simulated nonlinear conversion efficiency curves. Good correspondence was obtained between the measured curves and the ones that were expected according to simulations. From the measured phase-matching spectrum of the structure that contained two dislocations with even topological charges of $l_1 = 2$ and $l_2 = 2$ [Fig. 6(a)], one can see that one central significant peak of maximum conversion efficiency appeared at the wavelength that was originally intended to quasi-phase-match the SH process in a periodical structure without the dislocations. This shape of spectral response was also obtained in the past after the propagation of the FF beam through a structure that contained only one dislocation with an even topological charge. We wanted to examine these results in order to deduce a general conclusion. Therefore, we verified by numerical simulations and came to the conclusion that this kind of nonlinear spectral response is obtained with all other structures that contain any number of dislocations which are characterized by any even value of the topological charge. This is a generalization of a previous observation that was made for crystals with a single dislocation. The inset in Fig. 6(a) shows a simulation of the cumulative construction of the SH intensity, during the propagation of a 1.55 μm FF pump beam, which results in a maximum of conversion efficiency at the output of the crystal. The highest measured SH power was obtained for this structure, where for the wavelength of 1550.4 nm at the peak, we obtained for a pump power of 10.6 mW a power of 11.2 nW at the SH. Based on measurements of the SH power values for different FF pump power inputs, the experimental nonlinear conversion efficiency at this structure was $1.02 \times 10^{-2}\%/W$, while according to a simulation, a value of $2.34 \times 10^{-2}\%/W$ was obtained for the corresponding parameters to the experiment. We explain this difference between the results by the existence of deviations in the duty cycle of the actual created periodically poled domains compared to the designed modulation pattern in the crystal, where one-half of the length period was designed to be $+d_{ij}$ and the other half $-d_{ij}$. In order to test the effect of the duty cycle of the quasi-phase-matching modulation, we simulated for this structure the SH spectral efficiency curves for two additional modulation duty cycle values of 60% and 70%. We assumed that in each case, the duty cycle is constant throughout the crystal. The conversion efficiency, at the wavelength which provides phase matching, was reduced by 10% and 35% for the 60% and 70% duty cycles, respectively, relative to the optimal 50% duty cycle. This shows that the deviations in the poling pattern can explain the reduction in the measured SH signal. However, in all three simulations, the spectral shape was identical. These fixed deviations from the designed duty cycle do not explain the small wavelength shifts at the side peaks that were observed experimentally. According to the simulations, a spectral shift of the side peaks is not observed for different duty cycles, but only a decrease in the SH signal. Nonetheless, other deviations from the designed patterned structure, such as local deviations in the modulation duty cycle at different regions in the structure, as well as local variations in the quasi-phase-matching period may affect the measurement.

The spectral response for the structure that contained two dislocations, one with odd topological charge of $l_1 = 1$ and the second with even topological charge of $l_2 = 2$ [Fig. 6(b)], shows a different phase-matching spectrum. Two new pump wavelengths provided symmetric peaks of maximum conversion efficiency where between them a dip with a local minimum of conversion efficiency occurred at the wavelength of 1.55 μm that was originally meant to phase match the nonlinear process. The insets in Fig. 6(b) show simulations of the evolution of the SH intensity inside this crystal for two selected wavelengths of the pump beam. During the propagation of a 1.549-μm FF pump beam, a recovery of the SH intensity right after passing the first odd topological charge dislocation was noticed. In other words, despite the low back-conversion right after a propagation distance of one-third of the crystal's length, the propagation through the remaining two-thirds of the crystal's length, that includes the passing through the second even charge dislocation, leads to the left peak in the spectral efficiency curve. Unlike the top inset, for a pump wavelength of 1.55 μm, the SH intensity is being constructed until one-third of the crystal's length. A destruction of the generated SH beam starts from that point because of the odd topological charge dislocation. After a full back-conversion, the rebuilding of the SH intensity starts again only after a propagation distance of two-thirds of the crystal's length while passing through the even topological charge dislocation. This leads only to the dip that appears in the spectral efficiency curve. We also checked that the order of the two dislocations does not affect the efficiency spectrum.

The spectral efficiency curve for the structure that contained two dislocations with odd topological charges of $l_1 = 1$ and $l_2 = 1$ [Fig. 6(c)] shows that in this case two other pump wavelengths provide symmetrical global maxima. As opposed to the former structure or to a structure that contains only one odd topological charge dislocation at its center, between the two global peaks, a local maximum occurred at the wavelength of 1.55 μm of a lower conversion efficiency. The top inset in Fig. 6(c) shows a simulation of the recovery of the SH intensity during the propagation of a 1.548-μm pump beam after it passes the first odd topological charge dislocation. This creates the left global maximum in the efficiency spectrum. The bottom inset shows the total destruction and the recovery of the SH beam during the propagation of a 1.55-μm pump beam through the crystal. This leads to the local maximum in the efficiency spectrum. Also for these structures, we examined the relative conversion efficiencies according to the peaks for each of the two structures from Figs. 1(a) and 1(c) with reference to the case from Fig. 1(b). For the structure that included dislocations with $l_1 = l_2 = 1$, the measured relative conversion efficiency at the peak was $\eta_{\max}(l_1 = l_2 = 1)/\eta_{\max}(l_1 = l_2 = 2) = 0.57$, while the one obtained from a simulation was $\eta_{\max}(l_1 = l_2 = 1)/\eta_{\max}(l_1 = l_2 = 2) = 0.49$. For the structure that included dislocations with $l_1 = 1, l_2 = 2$, the measured relative conversion efficiency at the peak was $\eta_{\max}(l_1 = 1, l_2 = 2)/\eta_{\max}(l_1 = l_2 = 2) = 0.63$, while the one obtained in simulation was $\eta_{\max}(l_1 = 1, l_2 = 2)/\eta_{\max}(l_1 = l_2 = 2) = 0.47$. These results show that slightly higher efficiencies were

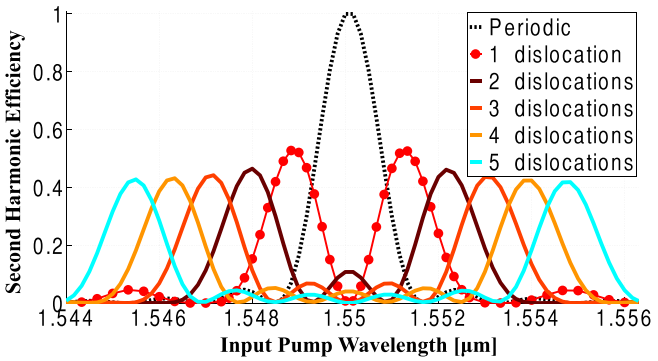

FIG. 7. (Color online) Spectral SH conversion efficiency for structures that contain multiple dislocations with odd topological charges. The simulations were performed for different structures with a growing amount of dislocations, where the designed patterns contained dislocations with topological charges of $l = 1$ and $l = 3$ arranged alternately.

measured in these two structures, relative to the structure with even topological charges, compared to the expected according to simulations. We think that the differences are caused by the deviations in the duty cycle in the fabricated structure with even topological charges, where also in the numerical conversion efficiency measurement we noticed that the expected value should have been higher. Nevertheless, we think that the relative efficiencies also present good correspondence between the experimental measurements and the theoretical expectations. By simulating the conversion efficiency spectrum of other structures that included a pair of edge dislocations, having higher odd charge values, we deduce that the same nonlinear spectral response as in Fig. 6(c) will characterize these type of structures.

When an FF pump with different wavelengths passes through a structure that contains a different number of dislocations with any odd topological charges, the phase-matching spectrum shows a completely different behavior in comparison to the case of multiple dislocations characterized by any even charges. The calculated nonlinear spectral response with additional odd topological charge dislocations to the structure is shown in Fig. 7. Therefore, we can deduce that for a growing number of odd topological charge dislocations we get a spectral response that is characterized by two symmetrical global maxima of conversion efficiency. Furthermore, the spectral distance between these two global peaks increases while more dislocations are added to the structure. In addition, new local peaks of maximum conversion efficiency emerge between the two global peaks. The number of these new local peaks is correlated with the number of the odd topological dislocations, where we get $N - 1$ local peaks for a total number of N dislocations in the structure. It should be noted that an FF pump with wavelength of 1.55 μm, which as one can see results in a global maximum of conversion efficiency in the dislocation-free structure, also results in a local maximum for structures with an even amount of odd dislocations, while a minimal SH power is obtained for structures with an odd amount of odd dislocations. The conversion efficiency decreases as the number of the dislocations increases because we simulated the beam propagation through crystals that have the same length. For that reason, the SH intensity cannot be constructed at the same rate because of smaller propagation distances before the first dislocation, in between the dislocations, and after the last dislocation. This is a generalization of a previous observation that was made for a single dislocation having an odd topological charge [28].

VI. CONCLUSION

We have studied the effects on the nonlinear scattering of electromagnetic waves, caused by embedded topological edge dislocations with different topological characters, in nonlinear photonic crystals. Specifically, we studied the changes in the spectrum of the SH signal generated in quadratic nonlinear photonic crystals as a result of dislocations in the nonlinear structures. The one-dimensional dislocation-free nonlinear photonic structure exhibits the familiar squared Sinc spectrum of the SH conversion efficiency. We examined nonlinear photonic crystals with a single edge dislocation, characterized by a fractional or an integer topological charge. In the case of a dislocation with a fractional topological charge, an asymmetry in the spectral nonlinear conversion efficiency response was observed. For various fractional topological charges we observed that the degree of asymmetry had been determined by the value of the fractional charge. Following this observation, we were able to realize and show that not only do these structures present such a clear dependence on parity, even more than that, the nonlinear conversion efficiency exhibits a periodic dependence on the topological charge value.

In addition, we examined nonlinear photonic crystals with multiple edge dislocations that had integer topological charges. We concluded that in the case of multiple dislocations, characterized by even topological charges, the nonlinear spectral response is identical to the response of the ideal, dislocation-free structure. This general result indicates that these added dislocations were almost invisible to the FF beam as they do not affect the nonlinear spectral response. Furthermore, we show that for structures with multiple edge dislocations, characterized by odd topological charges, the added dislocations stamp their fingerprints in the SH spectrum. These fingerprints are manifested by the rise of two new peaks of maximal efficiency, in addition to a series of local efficiency peaks that are governed by the total number of dislocations. By this result, one can use this method of investigating the signatures of dislocations on the nonlinear spectral response in order to deduce the number of dislocations that are present in a given structure.

Nonlinear photonic crystals pave the way to the study of the effects of dislocations on nonlinear scattering. As we presented, dislocations affect the familiar SH efficiency spectrum of a one-dimensional $\chi^{(2)}$ photonic crystal. It would be interesting to examine the effects of dislocations on photonic crystals that possess higher-order nonlinearities [32], as well as on two-dimensional quadratic photonic structures [33,34]. Furthermore, nonlinear scattering can occur in other media that exhibit different types of nonlinearities and with other types of waves such as fluid waves [35], acoustic waves [36], matter waves, or optical waves in other spectral ranges. Therefore, nonlinear scattering provides a new tool to study dislocations in materials by probing the material with one frequency and

observing the effect of the dislocation on its harmonics. In addition to its scientific merit, this characterization scheme can be attractive in cases in which the fundamental beam is absorbed or scattered in the material.

ACKNOWLEDGMENTS

This work was supported by the Israel Science Foundation, Grant No. 1310/13.

[1] G. I. Taylor, The mechanism of plastic deformation of crystals, Proc. R. Soc. A **145**, 362 (1934).
[2] N. F. Mott, Dislocations and the theory of solids, Nature (London) **171**, 234 (1953).
[3] R. Landauer, Spatial variation of currents and fields due to localized scatterers in metallic conduction, IBM J. **1**, 223 (1957).
[4] T. Ishida, K. Kakushima, T. Mizoguchi, and H. Fujita, Role of dislocation movement in the electrical conductance of nanocontacts, Sci. Rep. **2**, 623 (2012).
[5] Y. Oyama, Role of dislocation scattering on electron mobility in coalescent epitaxial lateral overgrowth layers of InP, J. Appl. Phys. **115**, 043722 (2014).
[6] R. L. Sproull, M. Moss, and H. Weinstock, Effect of dislocations on the thermal conductivity of lithium fluoride, J. Appl. Phys. **30**, 334 (1959).
[7] D. Kotchetkov, J. Zou, A. A. Balandin, D. I. Florescu, and F. H. Pollak, Effect of dislocations on thermal conductivity of GaN layers, Appl. Phys. Lett. **79**, 4316 (2001).
[8] D. Shilo and E. Zolotoyabko, Visualization of surface acoustic wave scattering by dislocations, Ultrasonics **40**, 921 (2002).
[9] A. Maurel, J.-F. Mercier, and F. Lund, Elastic wave propagation through a random array of dislocations, Phys. Rev. B **70**, 024303 (2004).
[10] J. F. Nye and M. V. Berry, Dislocations in wave trains, Proc. R. Soc. A **336**, 165 (1974).
[11] M. S. Soskin, V. N. Gorshkov, M. V. Vasnetsov, J. T. Malos, and N. R. Heckenberg, Topological charge and angular momentum of light beams carrying optical vortices, Phys. Rev. A **56**, 4064 (1997).
[12] A. Lopez Ariste, M. Collados, and E. Khomenko, Dislocations in magnetohydrodynamic waves in a stellar atmosphere, Phys. Rev. Lett. **111**, 081103 (2013).
[13] L. Korkidi, K. Barkan, and R. Lifshitz, in *Aperiodic Crystals: Analysis of Dislocations in Quasicrystals Composed of Self-assembled Nanoparticles*, edited by S. Schmid, R. L. Withers, and R. Lifshitz (Springer, Dordrecht, 2013), pp. 117–124.
[14] Y. V. Kartashov and L. Torner, Matter-wave soliton control in optical lattices with topological dislocations, Phys. Rev. A **74**, 043617 (2006).
[15] B. Freedman, G. Bartal, M. Segev, R. Lifshitz, D. N. Christodoulides, and J. W. Fleischer, Wave and defect dynamics in nonlinear photonic quasicrystals, Nature (London) **440**, 1166 (2006).
[16] B. Freedman, R. Lifshitz, J. W. Fleischer, and M. Segev, Phason dynamics in nonlinear photonic quasicrystals, Nat. Mater. **6**, 776 (2007).
[17] K. J. H. Law, A. Saxena, P. G. Kevrekidis, and A. R. Bishop, Stable structures with high topological charge in nonlinear photonic quasicrystals, Phys. Rev. A **82**, 035802 (2010).
[18] M. Padgett, J. Courtial, and L. Allen, Light's orbital angular momentum, Phys. Today **57**, 35 (2004).
[19] M. Uchida and A. Tonomura, Generation of electron beams carrying orbital angular momentum, Nature (London) **464**, 737 (2010).
[20] J. Verbeeck, H. Tian, and P. Schattschneider, Production and application of electron vortex beams, Nature (London) **467**, 301 (2010).
[21] A. Arie and N. Voloch, Periodic, quasi-periodic, and random quadratic nonlinear photonic crystals, Laser Photon. Rev. **4**, 355 (2010).
[22] C. B. Clausen and L. Torner, Spatial switching of quadratic solitons in engineered quasi-phase-matched structures, Opt. Lett. **24**, 7 (1999).
[23] J. P. Torres, A. Alexandrescu, S. Carrasco, and L. Torner, Quasi-phase-matching engineering for spatial control of entangled two-photon states, Opt. Lett. **29**, 376 (2004).
[24] C. B. Clausen and L. Torner, Self-bouncing of quadratic solitons, Phys. Rev. Lett. **81**, 790 (1998).
[25] X.-S. Song, F. Xu, and Y.-Q. Lu, Electromagnetically induced transparency-like transmission in periodically poled lithium niobate with a defect, Opt. Lett. **36**, 4434 (2011).
[26] N. Voloch-Bloch, K. Shemer, A. Shapira, R. Shiloh, I. Juwiler, and A. Arie, Twisting light by nonlinear photonic crystals, Phys. Rev. Lett. **108**, 233902 (2012).
[27] K. Shemer, N. Voloch-Bloch, A. Shapira, A. Libster, I. Juwiler, and A. Arie, Azimuthal and radial shaping of vortex beams generated in twisted nonlinear photonic crystals, Opt. Lett. **38**, 5470 (2013).
[28] S. Sharabi, N. Voloch-Bloch, I. Juwiler, and A. Arie, Dislocation parity effects in crystals with quadratic nonlinear response, Phys. Rev. Lett. **112**, 053901 (2014).
[29] J. A. Armstrong, N. Bloembergen, J. Ducuing, and P. S. Pershan, Interactions between light waves in a nonlinear dielectric, Phys. Rev. **127**, 1918 (1962).
[30] J. M. Jarem and P. P. Banerjee, *Computational Methods for Electromagnetic and Optical Systems* (Marcel Dekker, New York, 2000).
[31] I. Dolev, A. Ganany-Padowicz, O. Gayer, A. Arie, J. Mangin, and G. Gadret, Linear and nonlinear optical properties of MgO:LiTaO3, Appl. Phys. B **96**, 423 (2009).
[32] J. L. Bredas, C. Adant, P. Tackx, A. Persoons, and B. M. Pierce, Third-order nonlinear optical response in organic materials: Theoretical and experimental aspects, Chem. Rev. **94**, 243 (1994).
[33] V. Berger, Nonlinear photonic crystals, Phys. Rev. Lett. **81**, 4136 (1998).
[34] N. G. R. Broderick, G. W. Ross, H. L. Offerhaus, D. J. Richardson, and D. C. Hanna, Hexagonally poled Lithium Niobate: A two-dimensional nonlinear photonic crystal, Phys. Rev. Lett. **84**, 4345 (2000).
[35] O. M. Phillips, On the dynamics of unsteady gravity waves of finite amplitude, J. Fluid Mech. **9**, 193 (1960).
[36] A. P. Mayer, Surface acoustic waves in nonlinear elastic media, Phys. Rep. **256**, 237 (1995).